



Adaptive Catalysts for the Selective Hydrogenation of Bicyclic Heteroaromatics using Ruthenium Nanoparticles on a CO₂-Responsive Support

Yuyan Zhang, Sami El Sayed, Liqun Kang, Matthew Sanger, Thomas Wiegand, Philip G. Jessop, Serena DeBeer, Alexis Bordet,* and Walter Leitner*

Abstract: Ruthenium nanoparticles (NPs) immobilized on an amine-functionalized polymer-grafted silica support act as adaptive catalysts for the hydrogenation of bicyclic heteroaromatics. Whereas full hydrogenation of benzofuran and quinoline derivatives is achieved under pure H₂, introducing CO₂ into the H₂ gas phase leads to an effective shutdown of the arene hydrogenation while preserving the activity for the hydrogenation of the heteroaromatic part. The selectivity switch originates from the generation of ammonium formate species on the surface of the materials by catalytic hydrogenation of CO₂. The CO₂ hydrogenation is fully reversible, resulting in a robust and rapid switch between the two states of the catalyst adapting its performance in response to the feed gas composition. A variety of benzofuran and quinoline derivatives were hydrogenated to fully or partially saturated products in high selectivity and yields simply by altering the composition of the feed gas from H₂ to H₂/CO₂. The adaptive catalytic system thus provides controlled access to valuable products using a single catalyst rather than two specific and distinct catalysts with static reactivity.

Introduction

The hydrogenation of bicyclic heteroaromatics (e.g. benzofurans, quinolines, etc.) is an important transformation for the chemical industry, as the resulting compounds are key building blocks for the production of various fine chemicals,^[1] materials,^[2] and pharmaceuticals^[3] (see Figure 1 for examples). In the past decades, numerous efforts were dedicated to the development of homogeneous^[4] and heterogeneous^[5] catalysts capable of selectively accessing partially (only heterocycle hydrogenation)^[4a–h,5a–d,f,g] or fully (heterocycle + arene hydrogenation)^[4i,5e,h] saturated heterocyclic compounds. The production of these two classes of products typically requires the use of two distinct classes of catalysts, however. For example, the selective hydrogenation of benzofuran to dihydrobenzofuran requires catalysts possessing the ability to hydrogenate the heteroaromatic furan ring while leaving the six-membered aromatic ring untouched. This can be achieved using homogeneous Ru-NHC complexes^[4d,f,g] and monometallic^[5b,f,g] or bimetallic^[5e] nanoparticles in ionic liquid environments. In contrast, full hydrogenation of benzofuran to octahydrobenzofuran necessitates the additional hydrogenation activity for 6-membered aromatic carbocycles. Heterogeneous catalysts based on noble metal NPs are typically used to achieve full hydrogenation.^[5h] Thus, while state-of-the-art catalysts present often outstanding properties regarding their dedicated tasks, their performance is typically optimized to provide maximum activity and selectivity toward one class of product only.

An alternative approach relies on the design of adaptive catalytic systems allowing to switch the performance of a given material by an external stimulus in a fully reversible, robust and rapid manner.^[6] Thus, the same catalyst in a single reactor unit can produce different products for example in response to the dynamics of alternative energy sources, quality variations of chemical feedstocks, and rapidly changing market demand for products. Such adaptive catalytic systems can provide innovative processing options to enable decentralized and customized production.^[7] Here, we report a rationally designed catalytic system capable of hydrogenating bicyclic heteroaromatics selectively to partially as well as fully saturated products in a fully adaptive manner.

Recently, we reported a multifunctional catalytic system composed of Ru NPs immobilized on tertiary amine-

[*] Dr. Y. Zhang, Dr. L. Kang, Prof. Dr. T. Wiegand, Prof. Dr. S. DeBeer, Dr. A. Bordet, Prof. Dr. W. Leitner
 Max Planck Institute for Chemical Energy Conversion, Department of Molecular Catalysis
 Stiftstraße 34–36, 45470 Mülheim an der Ruhr (Germany)
 E-mail: alexis.bordet@cec.mpg.de
 walter.leitner@cec.mpg.de

Dr. S. El Sayed, Prof. Dr. T. Wiegand, Prof. Dr. W. Leitner
 Institut für Technische und Makromolekulare Chemie, RWTH Aachen University
 Worringerweg 2, 52074 Aachen (Germany)

M. Sc. M. Sanger, Prof. Dr. P. G. Jessop
 Department of Chemistry, Queen's University
 Kingston, Ontario (Canada)

© 2023 The Authors. Angewandte Chemie International Edition published by Wiley-VCH GmbH. This is an open access article under the terms of the Creative Commons Attribution License, which permits use, distribution and reproduction in any medium, provided the original work is properly cited.

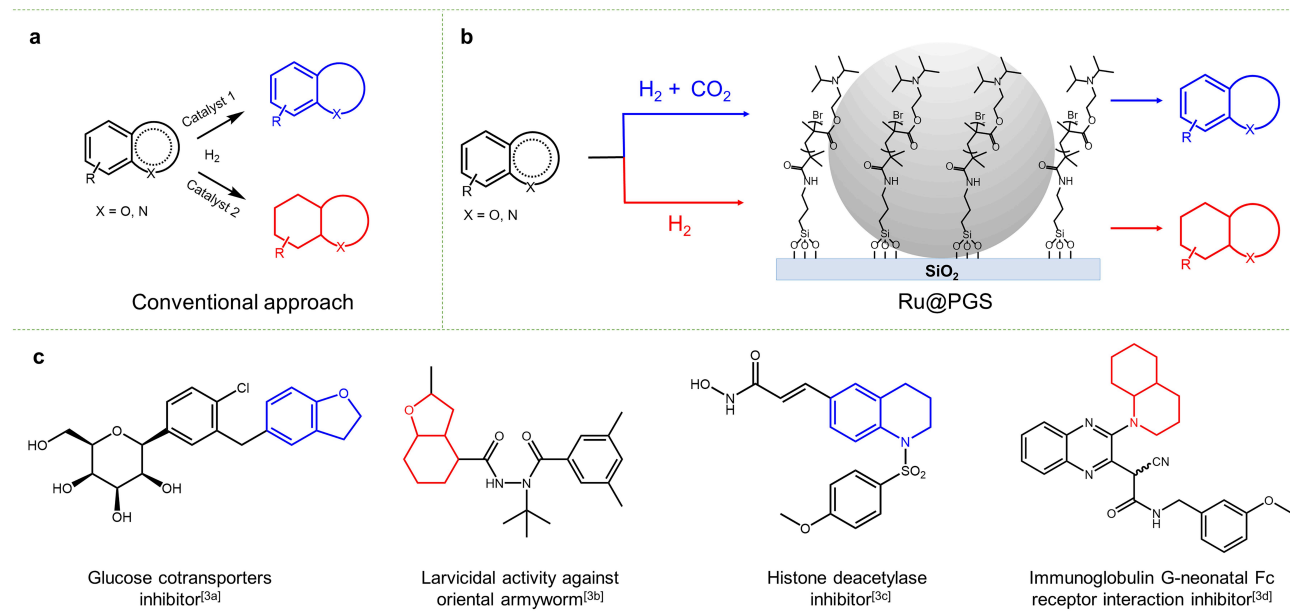


Figure 1. Illustration of (a) the conventional approach to the hydrogenation of bicyclic heteroaromatics, (b) the adaptive hydrogenation of bicyclic heteroaromatics using Ru@PGS with CO₂ as a molecular trigger, (c) examples of potential applications of partially or fully saturated benzofuran and quinoline derivatives.

functionalized polymer-grafted silica (PGS).^[8] The resulting Ru@PGS catalyst was found to respond in an adaptive manner to the feed gas composition in the hydrogenation of ketone-containing furan derivatives. While full hydrogenation was observed under H₂, ketone hydrogenation activity was selectively shut down in the presence of a mixture of H₂/CO₂. The reversible formation of ammonium formate species at the surface of the Ru NPs was inferred from spectroscopic data to act as a molecular trigger for the selectivity switch.

Herein, we apply this adaptive catalytic system to the hydrogenation of benzofurans, another class of furan-containing compounds that find widespread application in the fine chemical and pharmaceutical industry.^[3a,b] In this case, the use of CO₂ as a molecular trigger is explored to switch the hydrogenation activity of the Ru NPs for the 6-membered arene ring. The concept is then expanded to nitrogen-containing heterocycles and a wide variety of quinoline derivatives is also partially or fully hydrogenated in an adaptive manner (Figure 1).

Results and Discussion

The Ru@PGS catalyst was prepared following a procedure recently reported by our team.^[8] Synthesis of the tertiary amine-functionalized PGS support material involved the molecular modification of commercial amorphous SiO₂ by silanization and surface-initiated atom transfer radical polymerization.^[9] Successful chemisorption of the amine-functionalized polymer on SiO₂ was demonstrated by N₂ adsorption and ²⁹Si solid state NMR in a previous study.^[8] The immobilization of Ru NPs on PGS was accomplished

using our bottom-up organometallic approach known to produce small and well-defined NPs on functional supports.^[5b,10] In brief, the PGS support was loaded with Ru by wet impregnation with a solution of [Ru(2-methylallyl)₂-(cod)] (where cod = 1,5-cyclooctadiene) in tetrahydrofuran (THF). After removal of the solvent *in vacuo*, the dried powder was subjected to an atmosphere of H₂ (25 bar) at 100 °C for 18 h, giving the Ru@PGS material as a fine black powder. Ru@SiO₂ was prepared following the same approach to serve as reference catalyst without surface modification (see Supporting Information for detailed procedures). The Ru@PGS material was characterized using elemental analysis (0.82 mmol g⁻¹ Ru), N₂ physisorption (BET surface area = 68 m² g⁻¹), and electron microscopy (Figure 2), giving results consistent with our previous study.^[8] In particular, bright field scanning transmission electron microscopy images (BF-STEM, Figure 2b-c) showed small and fairly well dispersed NPs with an average size of 1.7 ± 0.7 nm (size distribution in Figure S1) exhibiting a nearly spherical shape. Lattice spacings of the NPs were determined from the Fast Fourier Transformation (FFT, insert Figure 2c) of the BF-STEM image, showing lattice distances of 2.34 Å, 2.14 Å and 2.05 Å which correspond well to the (110), (002) and (111) facets of *hcp* ruthenium (P6₃/mmc), respectively. High angle annular dark field STEM and elemental mapping using energy dispersive X-ray spectroscopy (HAADF-STEM & EDX mapping, Figure 2d–g, summary of EDX spectrum provided in Figure S2) showed that Ru (Figure 2e) and Br (Figure 2f) are fairly well dispersed on the SiO₂ support (Si mapping Figure 2g), indicating that the polymer, SiO₂ support, and Ru NPs are in close proximity. The reference Ru@SiO₂ material was characterized by elemental analysis, N₂ physisorption, and

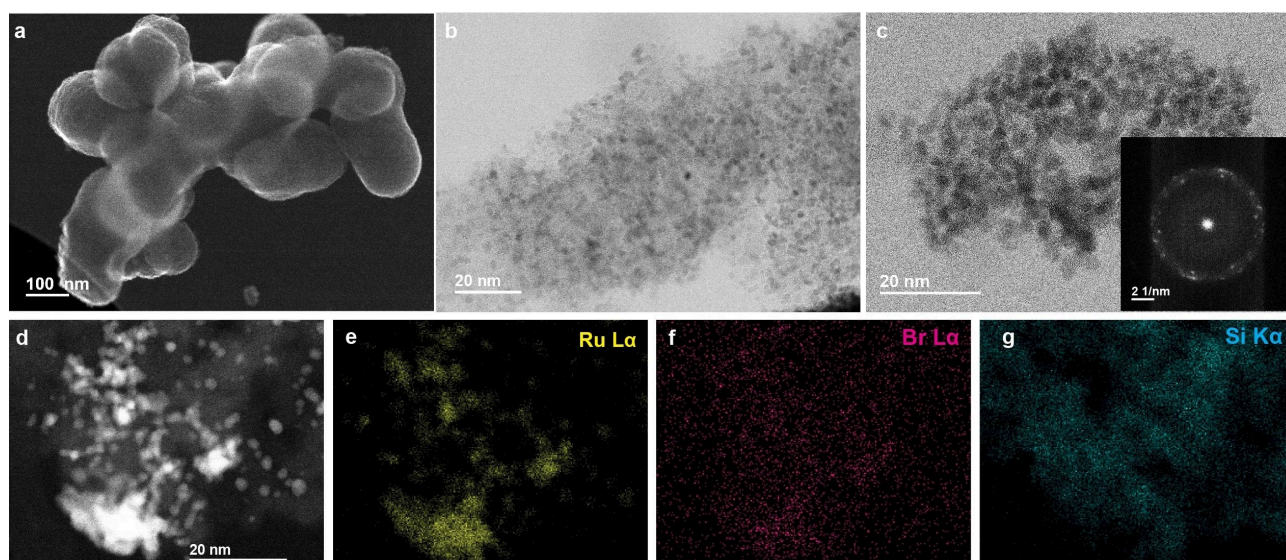


Figure 2. Characterization of Ru@PGS by electron microscopy. (a) Secondary electron SEM images (SE-SEM); (b, c) Bright field STEM image (BF-STEM), insert represents Fast Fourier Transform analysis; (d) HAADF-STEM image and corresponding (e-g) EDS elemental mapping of (e) Ru, (f) Br, and (g) Si in Ru@PGS structure using Ru L α (2.56 keV), Br L α (1.48 keV) and Si K α (1.74 keV) fluorescence lines respectively.

HAADF-STEM, showing a Ru loading of 0.79 mmol g^{-1} , a BET surface area of $404 \text{ m}^2 \text{ g}^{-1}$, and Ru NPs of $1.7 \pm 0.5 \text{ nm}$ (Figure S3), respectively.

The hydrogenation of benzofuran (**1a**) was selected as a model reaction to probe the reactivity of the Ru@PGS catalyst with pure hydrogen (H_2) or hydrogen in the presence of CO_2 (H_2/CO_2) as the gas feed (Table 1). Ru@SiO₂ was used as a reference catalyst for comparison. The hydrogenation of benzofuran (**1a**) can proceed following two possible reaction pathways: (1) the most common pathway starts with hydrogenation of the furan ring to

produce 2,3-dihydrobenzofuran (**1b**), followed by hydrogenation of the arene ring to give octahydrobenzofuran (**1d**); (2) alternatively, the arene ring can be hydrogenated first leading to hexahydrobenzofuran (**1c**), prior to furan ring hydrogenation to give **1d**. The catalytic reactions were performed under batch conditions using stainless-steel high-pressure autoclaves equipped with magnetic stir bars. The solvent, amount of substrate, and reaction time were set to *n*-butanol, 25 equivalents with respect to total Ru loading, and 16 h, respectively. A temperature of 80°C and a H_2 partial pressure of 30 bar (total pressure of 45 bar for H_2/CO_2 , with a 2:1 ratio) were selected after a brief parameter optimization (Table S1).

Starting with Ru@PGS and H_2 as feed gas, **1a** was completely hydrogenated to give product **1d** in 92 % yield (Table 1, Entry 1), corresponding to the expected reactivity of Ru NPs under such conditions.^[11] Switching the feed gas to a mixture of H_2/CO_2 and applying the identical partial pressure of H_2 led to the formation of the partially saturated product **1b** in high yield (83 %, Table 1, Entry 2), without any trace of **1c**. In contrast, the reactivity of a reference Ru@SiO₂ catalyst without molecular modifier was not affected by the presence of CO_2 in the feed gas, and quantitative yields (97 %) of **1d** were obtained under H_2 and a mixture of H_2/CO_2 (Table 1, Entries 3–4).

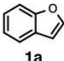
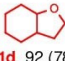
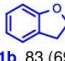
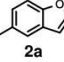
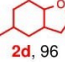
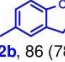
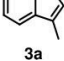
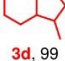
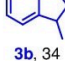
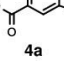
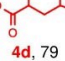
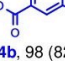
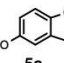
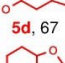
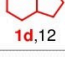
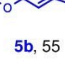
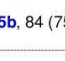
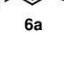

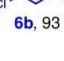
In a recent study, we have shown that the reactivity of Ru NPs in Ru@PGS could be switched in the presence of H_2/CO_2 due to the reversible formation of ammonium formate species on the catalyst, resulting in the suppression of ketone hydrogenation activity.^[8] The present results indicate that the same molecular trigger can also be effective to control arene reduction during benzofuran hydrogenation, demonstrating the broader applicability of the concept. Indeed, the formation of ammonium formate species on Ru@PGS treated with H_2/CO_2 (45 bar, 2:1) under the

Table 1: Hydrogenation of **1a** using Ru@PGS under H_2 or H_2/CO_2 as feed gas.

Entry	Catalyst	$p\text{H}_2$ [bar]	$p\text{CO}_2$ [bar]	Conv. [%]	Y_{1d} [%] ^[a]	Y_{1b} [%] ^[a]
1	Ru@PGS	30	—	> 99	92	2
2		30	15	97	12	83
3	Ru@SiO ₂	30	—	> 99	97	0
4		30	15	> 99	97	0
5 ^[b]		30	—	90	7	77

Reaction conditions: Ru@PGS or Ru@SiO₂ (0.026 mmol Ru), substrate (0.65 mmol, 25 eq.), *n*-butanol (0.65 mL), 80°C , 16 h, Conv. = conversion, ^[a] Y = yield, determined by GC-FID using tetradecane as an internal standard, rest = 2-ethylphenol. ^[b]Additive: diisopropyl(ethyl)ammonium formate (DIPEF), 0.025 eq. with respect to **1a**, DIPEF/Ru = 0.63.

Table 2: Hydrogenation of benzofuran derivatives using Ru@PGS catalysts under H₂ or H₂/CO₂.

#	Substrate (Xa)	T (°C)	CO ₂ switched OFF			CO ₂ switched ON		
			pH ₂ (bar)	Conv. (%)	Y(main product) ^[a] (%)	pH ₂ /CO ₂ (bar)	Conv. (%)	Y(main product) ^[b] (%)
1		80	30	99	 1d , 92 (78)	30/15	97	 1b , 83 (69)
2		100	80	>99	 2d , 96	80/5	95	 2b , 86 (78)
3		120	30	>99	 3d , 99	30/15	84	 3b , 34
4		100	80	>99	 4d , 79	80/15	>99	 4b , 98 (82)
5		80	30	>99	 5d , 67  1d , 12	30/5 100/5	55 88	 5b , 55  5b , 84 (75)
6		80	80	>99	 6d , 93	80/5	>99	 6b , 93

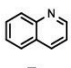
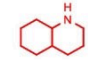
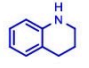
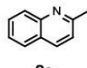
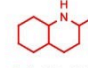
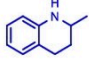
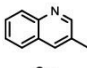
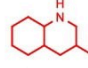
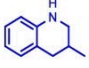
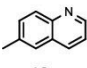
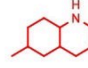
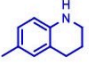
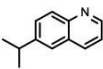
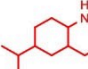
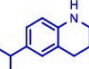
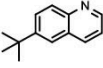
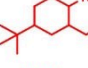
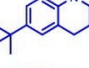
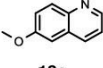
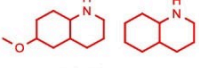
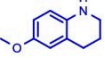
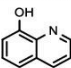
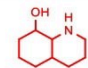
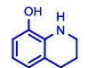
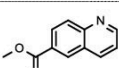
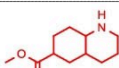
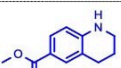
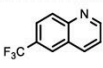
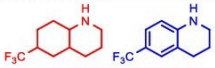
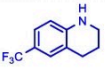
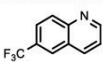
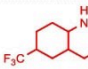
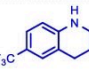
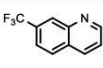
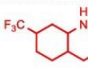
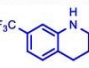
Reaction conditions: Ru@PGS (0.026 mmol Ru), substrate (0.65 mmol, 25 eq.), *n*-butanol (0.65 mL), 16 h, Conv. = conversion, Y = yield. Conversions and product yields determined by GC-FID using tetradecane as the internal standard. ^[a]Rest = products Xb. ^[b]Rest = products Xd. Isolated yields are given in parentheses.

standard conditions of the present study (80 °C, 16 h) in deuterated methanol was confirmed by ¹H and ¹³C NMR spectroscopy (Figure S4). Analysis of the reaction mixture containing the catalyst in suspension showed signals characteristic of ammonium formate species at 8.4 ppm (¹H NMR spectrum) and 165 ppm (¹³C NMR spectrum). In addition, solid-state ¹³C cross polarization magic angle spinning (¹³C CP-MAS) NMR analysis of the Ru@PGS material after the reaction with H₂/CO₂ revealed a new signal at 164 ppm, thus confirming the presence of ammonium formate species on the spent catalyst surface (Figure S5). Furthermore, diisopropyl(ethyl)ammonium formate (DIPEF) when applied as an additive in the hydrogenation of **1a** catalyzed by the reference catalyst Ru@SiO₂ under pure H₂ changed the selectivity (Table 1, Entry 5), clearly demonstrating the suppression of arene hydrogenation by presence of the ammonium formate. A mixture of **1b** (77 %) and **1d** (7 %) was obtained under these conditions with a DIPEF:Ru ratio of 0.63 (Table S2), which is close to the amine:Ru ratio present on the Ru@PGS catalyst (0.69). Using less DIPEF resulted in a less effective selectivity switch, while adding it in excess decreased the total catalytic activity (Table S2). Interestingly, the amine structure of the ammonium formate species used as additives was found to have also a strong influence on the extent of the selectivity switch observed (Table S3), with tertiary bulky amines being particularly suitable for the present application.

To gain further insight into the reactivity of Ru@PGS for the hydrogenation of **1a**, time profiles were recorded using H₂ or H₂/CO₂ as feed gas (Figure 3).

Under H₂, **1a** was quickly hydrogenated to **1b** in the first hour (initial rate = 0.62 mol L⁻¹ h⁻¹), which was further converted into **1d** over time (initial rate = 0.15 mol L⁻¹ h⁻¹) in a typical profile for the sequential hydrogenation of **1a** (Figure 3a). The hydrogenation of **1a** to **1b** still occurred smoothly under H₂/CO₂, albeit at a slightly reduced rate (initial rate = 0.40 mol L⁻¹ h⁻¹), which further decreased over time. Arene hydrogenation, however, was essentially shut down reducing the rate by roughly one order of magnitude (initial rate = 0.02 mol L⁻¹ h⁻¹), and even suppressing it after 4 h. Thus, the yield of **1d** remained below 10 % even after 24 h of reaction (Figure 3b). Interestingly, the decrease in **1a** = > **1b** rate, and suppression of the **1b** = > **1d** step after a few hours of reaction is presumably due to the progressive establishment of formate species at the surface of Ru NPs, decreasing the availability of free space on the surface, and preventing the re-adsorption of **1b**. The adsorption capacity of **1b** on Ru@PGS treated under H₂/CO₂ (0.34 mg mg_{Ru}⁻¹ on Ru@PGS-[HNEt₂]⁺[HCOO]⁻) was found much lower than on Ru@PGS treated under H₂ (1.37 mg mg_{Ru}⁻¹ on Ru@PGS-NEt₂), supporting this hypothesis (see Supporting Information for experimental details). In sharp contrast, the kinetic profile obtained with Ru@SiO₂ was not affected by the composition of the feed gas (Figure S6).

Table 3: Hydrogenation of quinoline derivatives using Ru@PGS under H₂ or H₂/CO₂.

#	Substrate (Xa)	T (°C)	CO ₂ switched OFF			CO ₂ switched ON		
			pH ₂ (bar)	Conv. (%)	Y(main product) ^[a] (%)	pH ₂ /CO ₂ (bar)	Conv. (%)	Y(main product) ^[b] (%)
1	 7a	100	30	>99	 7d, 98 (90)	30/15	>99	 7b, 86 (63)
2	 8a	100	30	>99	 8d, 99 (92)	30/15	99	 8b, 89 (73)
3	 9a	120	50	>99	 9d, 85	50/30	97	 9b, 88
4	 10a	100	30	>99	 10d, 99 (93)	30/15	>99	 10b, 94 (79)
5	 11a	120	30	>99	 11d, 99	30/15	>99	 11b, 88
6	 12a	120	30	>99	 12d, 78	30/15	>99	 12b, 99
7	 13a	100	30	>99	 13d/7d, 53/47	30/15	>99	 13b, 95 (81)
8	 14a	120	50	>99	 14d, 94	50/15	>99	 14b, 99
9	 15a	120	50	>99	 15d, 78	50/15	>99	 15b, 94 (78)
10	 16a	100	30	>99	 16d/16b, 32/68	30/15	>99	 16b, 97
11	 16a	120	50	>99	 16d, 80 ^c	50/15	>99	 16b, 92
12	 17a	120	50	>99	 17d, 90 ^d	50/15	>99	 17b, 97

Reaction conditions: Ru@PGS (0.026 mmol Ru), substrate (0.65 mmol, 25 eq.), *n*-butanol (0.65 mL), 16 h, Conv. = conversion, Y = yield. Conversions and product yields determined by GC-FID using tetradecane as the internal standard. ^[a] Rest = products Xb. ^[b] Rest = the corresponding 5,6,7,8-tetrahydroquinoline. ^[c] side product: 1-butyl-7-(trifluoromethyl)decahydroquinoline; ^[d] side product: 1-butyl-6-(trifluoromethyl)decahydroquinoline. Isolated yields are given in parentheses. Yields of products Xc < 5%.

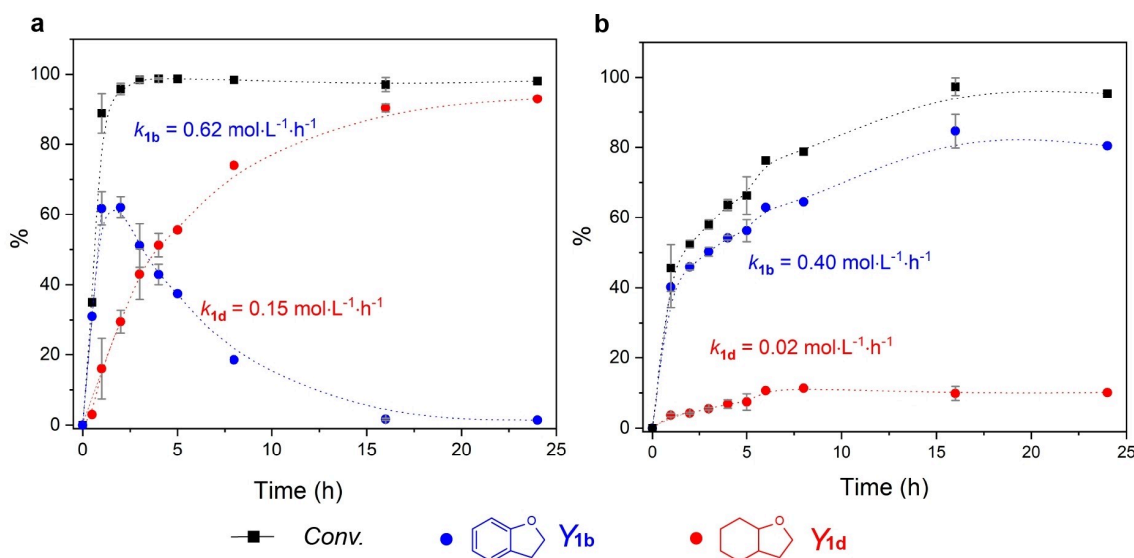


Figure 3. Time profiles of the hydrogenation of **1a** using Ru@PGS under (a) H_2 and (b) H_2/CO_2 . Reaction conditions: Ru@PGS (0.026 mmol Ru), substrate (0.65 mmol, 25 eq.), *n*-butanol (0.65 mL), 80°C , (a) H_2 (30 bar) or (b) H_2/CO_2 (45 bar, 2:1), Conv. = conversion, Y = yield. Product yield determined by GC-FID using tetradecane as the internal standard. Data points are average values of three experiments and error bars represent standard deviations.

As the hydrogenation of CO_2 to formic acid is known to be an equilibrium reaction, we evaluated the reversibility of the formate-induced selectivity switch (Figure 4a) between the formation of **1b** and **1d** using the Ru@PGS catalyst in alternating cycles of H_2 and H_2/CO_2 as feed gas (Figure 4b, and Supporting Information for detailed procedure). Under standard conditions, high yields of **1d** (88–92 %) under H_2 and of **1b** (73–80 %) under H_2/CO_2 were observed in six consecutive alternating runs without sign of deactivation, demonstrating that the switching of the Ru@PGS catalyst is

fully and repeatably reversible. The reversibility of the formate species formation was demonstrated by liquid-state ^1H NMR (Figure S7) and solid-state ^{13}C CP-MAS NMR (Figure S8), which showed that the formate species are absent in the first cycle under H_2 (Figure S7a and S8a), formed under H_2/CO_2 (Figure S7b and S8b, signals at 8.4 and 164 ppm, respectively), and effectively decomposed when the feed gas is switched back to H_2 (Figure S7c and S8c), with CO_2 being released in the process (Figure S9).

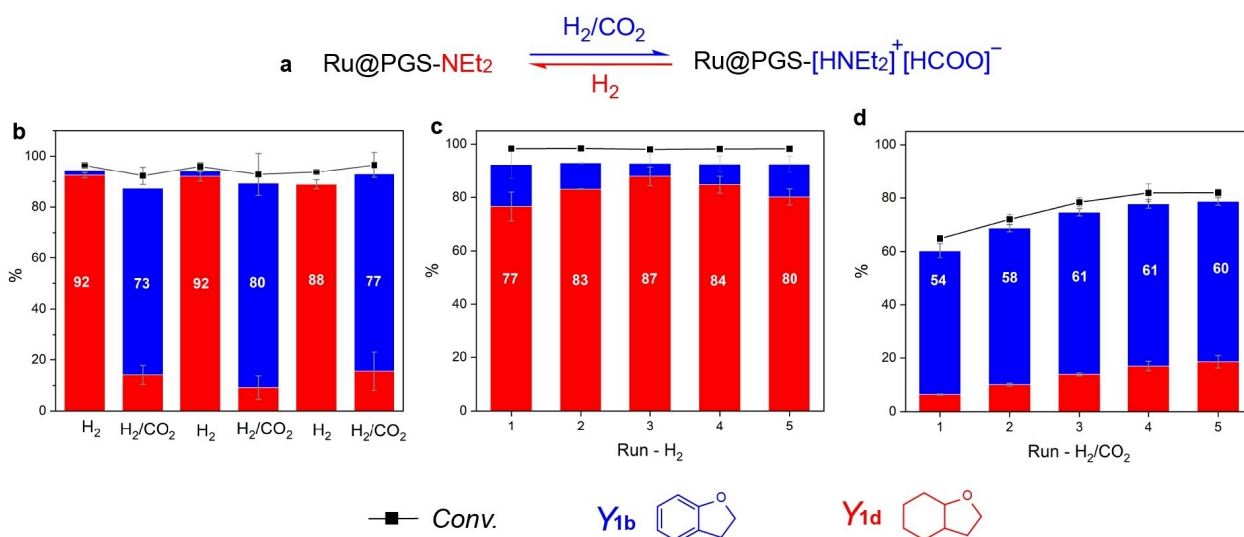


Figure 4. (a) Proposed trigger for the selectivity switch using Ru@PGS, (b) reversibility, and recycling studies for the hydrogenation of **1a** under (c) H_2 and (d) H_2/CO_2 using Ru@PGS. Reaction conditions for reversibility: Ru@PGS (0.026 mmol Ru), substrate (0.65 mmol, 25 eq.), *n*-butanol (0.65 mL), H_2 (30 bar) or H_2/CO_2 (45 bar, 2:1), 80°C , 16 h. For the recycling study, the reaction time is 5 h. Product yield determined by GC-FID using tetradecane as the internal standard. Data points are average values of two to four experiments and error bars represent standard deviations.

In addition, the reusability and robustness of Ru@PGS were further investigated through recycling experiments (detailed procedure in SI). The conditions were set to remain below 100 % conversion (reaction time 5 h), and five consecutive runs were performed with H₂ (Figure 4c) and with H₂/CO₂ (Figure 4d). Conversion and product distributions remained constant under pure hydrogen, while a slight increase of the yield of arene hydrogenation product was observed under H₂/CO₂. This may reflect a slight accumulation of partially hydrogenated product on the catalyst material being carried over from one cycle to the other.

Electron microscopy of Ru@PGS after catalysis under H₂ (Figure 5b, Figure S10a and Figure S11a) or H₂/CO₂ (Figure 5c, Figure S10b and Figure S11b) did not show substantial change in the size, dispersion, and crystal structure of Ru NPs as compared to the fresh catalyst (Figure 5a, Figure 2). In addition, X-ray absorption near edge structure (XANES) and Ru K-edge extended X-ray absorption fine structure (EXAFS) spectra of Ru@PGS before and after catalysis were very similar (Figure 5d-e). The absorption edge positions of the fresh and spent Ru@PGS catalysts are nearly identical (at 22122.0 eV). This is approximately 2.6 eV higher than that of Ru(0) in Ru metal foil (22119.4 eV), but 5.3 eV lower than that of Ru(IV) in RuO₂ (22127.3 eV). This suggests that Ru is mainly in the metallic state in Ru@PGS materials, with only traces of oxidation. In addition, for both Ru–O and Ru–Ru in the first coordination shell, neither the coordination number nor the bond length was changed noticeably under H₂ or H₂/CO₂ as the feed gas (Table S4, Figure S12), indicating that no substantial growth or aggregation of Ru

NPs occurred. This is consistent with statistical results obtained from electron microscopy (Figure 5a–c). Leaching of Ru or Br in solution during catalysis was found to be negligible (Table S5). BET surface areas (Table S6) of spent Ru@PGS catalysts used under H₂ (54 m²g^{−1}) or H₂/CO₂ (66 m²g^{−1}) were very similar to that of fresh Ru@PGS (68 m²g^{−1}), supporting the absence of noticeable polymer leaching during catalysis. These results demonstrate the robustness of the Ru@PGS catalyst and the absence of irreversible structural or electronic modifications arising from its use under different feed gas, highlighting again its adaptivity.

In contrast, Ru NPs were found more aggregated on Ru@SiO₂ after catalysis, and their size increased to 2.3 ± 0.7 nm (Figure S13). Noticeable Ru leaching (from 0.79 to 0.71 mmol g^{−1}) was also observed by ICP-OES (Table S7). These results suggest that the amine-functionalized polymeric modifier of the PGS support has a beneficial stabilizing effect on the Ru NPs.

The versatility of this selectivity switch suppressing arene hydrogenation through the addition of CO₂ to the H₂ feed gas was investigated by expanding the substrate scope to a variety of commercially available benzofuran derivatives (Table 2). Satisfyingly, hydrogenation selectivity could be controlled using CO₂ as the molecular trigger for these substrates as well under optimized conditions (optimization steps in Table S8), leading to the selective production of either octahydrobenzofurans under H₂ or dihydrobenzofurans under H₂/CO₂ under otherwise identical conditions.

Under H₂ as feed gas, Ru@PGS catalyzed the complete hydrogenation of substrates **1a–5a** (Table 2, Entries 1–5) to

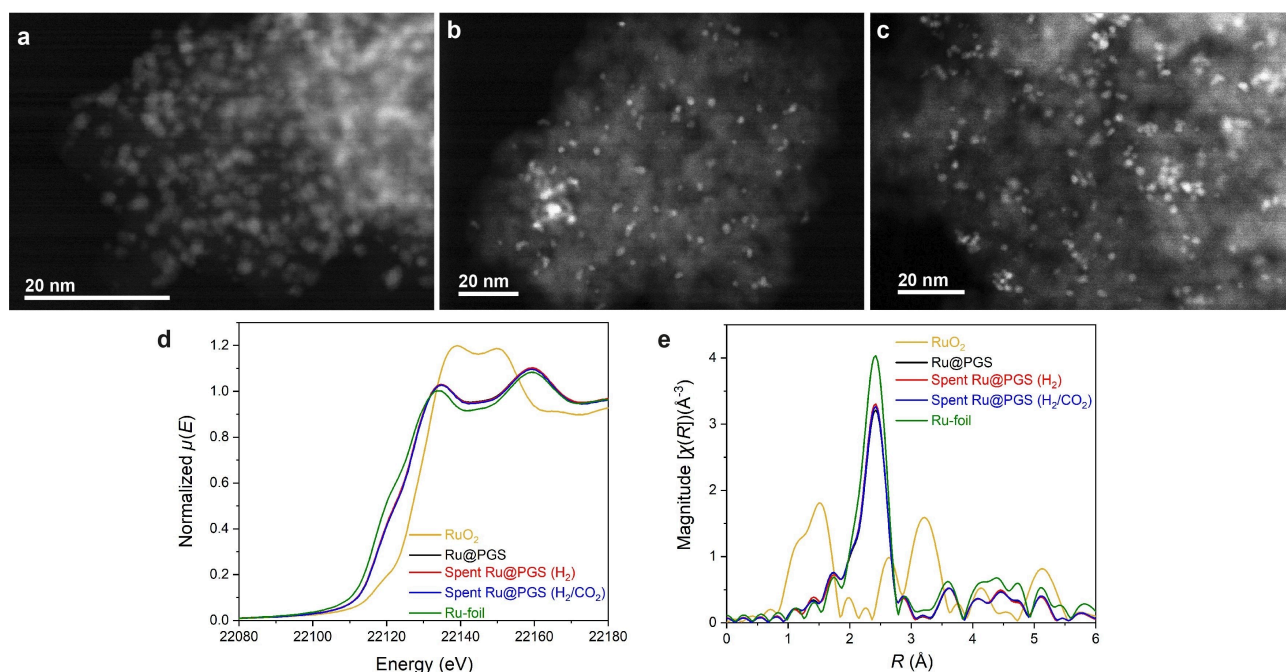


Figure 5. Characterization of Ru@PGS before and after catalysis. HAADF-STEM images of (a) fresh Ru@PGS, and Ru@PGS after hydrogenation of **1a** under (b) H₂ and (c) H₂/CO₂ as feed gas, (d) Ru K-edge XANES spectra (normalized) and (e) Ru K-edge *k*²-weighted R-space FT-EXAFS spectra (plot in FT magnitude without phase correction) of fresh Ru@PGS catalyst Ru@PGS after hydrogenation of **1a** under H₂ or H₂/CO₂ as feed gas.

produce **1d–5d** in high yields (67–99 %). With substrate **5a** (Table 2, Entry 5), partial hydrogenolysis of the methoxy functionality occurred, consistent with previous observations with Ru NPs catalysts.^[5b,12] When applying H₂/CO₂ as feed gas, the aromaticity of the arene ring was effectively maintained in products **1b–2b** and **4b–5b**, with yields ranging from 83 to 98 %. The partial pressure of CO₂ was optimized for each substrate individually to maximize the yields of desired products **Xb**. Substitution in position 3 (substrate **3a**) resulted in reduced selectivity under H₂/CO₂, giving a poor yield of **3b** (34 %) together with **3d** (39 %) and 2-isopropylphenol (10 %) as by-products. In addition, no selectivity switch could be observed in the hydrogenation of substrate **6a**, as full hydrogenation could not be reached even under pure H₂ (Table 2, Entry 6). Among these products, **4d** is used for example as a building block for the synthesis of inhibitors of mutant IDH enzymes (involved in cancers),^[13] while **4b** can be employed as a starting material

in the preparation of 1,3,4-oxadiazole derivatives as novel inhibitors of glycogen synthase kinase-3 β .^[1c]

Next, the hydrogenation of quinoline derivatives using Ru@PGS was explored, taking quinoline (**7a**) as a model substrate. This choice was motivated both by the synthetic interest of this transformation to access valuable building blocks,^{[14],[4c]} and by the interest in testing the adaptivity of Ru@PGS for other substrates than furan-containing compounds. The hydrogenation of **7a** to the fully hydrogenated decahydroquinoline (**7d**) product can proceed through two partially saturated intermediates (1,2,3,4-tetrahydroquinoline (**7b**) and 5,6,7,8-tetrahydroquinoline (**7c**)) (Figure 6a). At 100 °C (temperature optimization in Table S9) and otherwise standard conditions, **7a** was fully hydrogenated over Ru@PGS to **7d** (97 % yield) under H₂ (Table S10, Entry 1). Introducing CO₂ in the hydrogen feed gas resulted in a selectivity switch, and **7b** was produced in high yield (86 %, Table S10, Entry 2), with small amounts of **7c**.

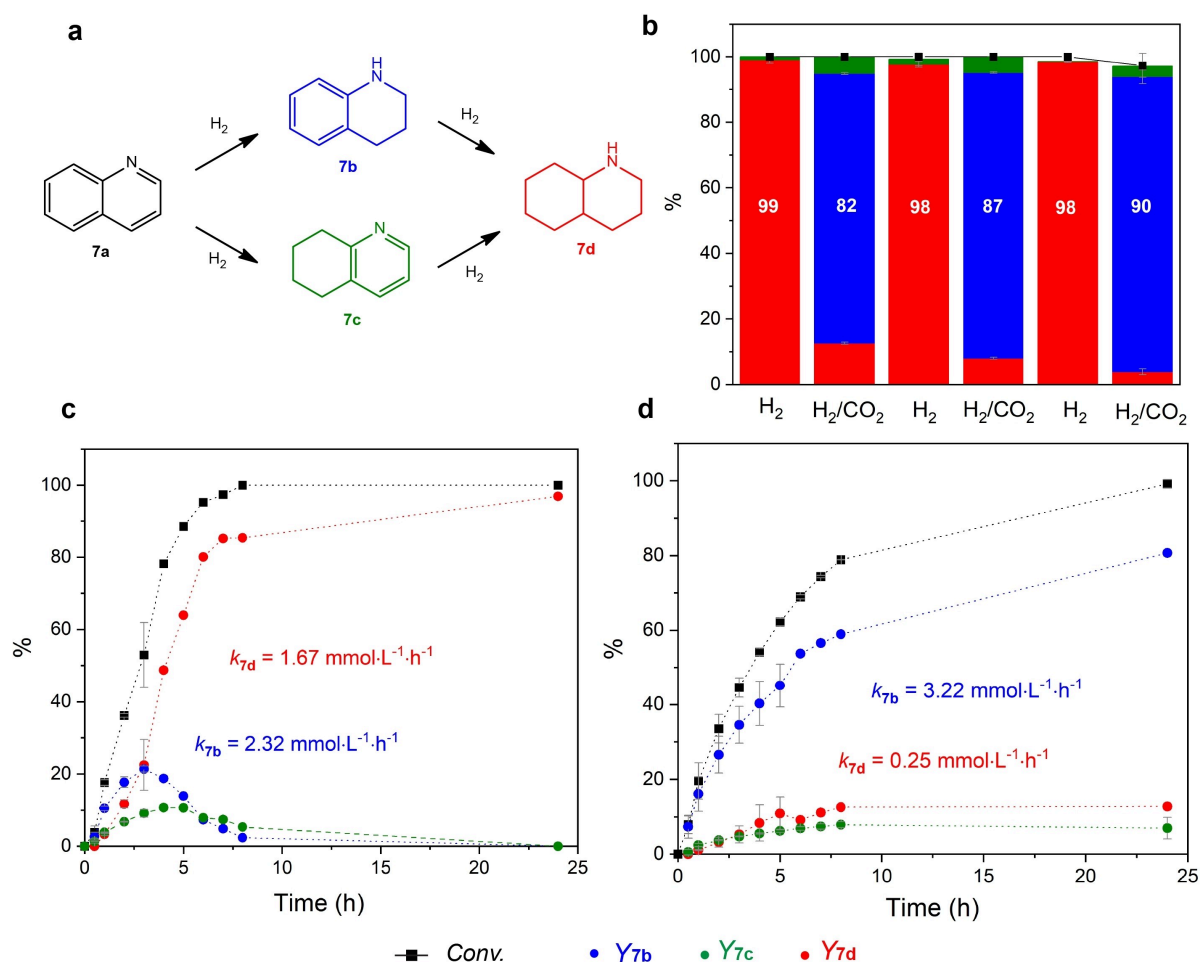


Figure 6. Hydrogenation of quinoline (**7a**) using Ru@PGS under H₂ or H₂/CO₂. (a) General reaction scheme; (b) reversibility study; time profiles under (c) H₂ and (d) H₂/CO₂. Reaction conditions for reversibility study: Ru@PGS (0.026 mmol Ru), substrate **7a** (0.65 mmol, 25 eq.), *n*-butanol (0.65 mL), H₂ (30 bar) or H₂/CO₂ (45 bar, 2:1), 100 °C, 16 h. Reaction conditions for time profiles: Ru@PGS (0.074 mmol Ru), substrate **7a** (1.7 mmol, 17 eq.), *n*-butanol (65 mL), 100 °C, H₂ (30 bar) or H₂/CO₂ (45 bar, 2:1), Conv. = conversion, Y = yield. Conversions and product yields determined by GC-FID using tetradecane as the internal standard. Data points are average values of two to three experiments and error bars represent standard deviations.

Interestingly, with this substrate, a moderate selectivity switch was also observed with Ru@SiO₂ (Table S10, Entries 3–4). In this case, formate species were detected by ¹H NMR after reaction under H₂/CO₂ (Figure S14), and come from a reaction between product **7d** and formic acid generated in situ by CO₂ hydrogenation (Figure S15–16).

Satisfyingly, alternating H₂ and H₂/CO₂ as feed gas in six consecutive cycles gave consistently **7d** under H₂ or **7b** under H₂/CO₂ with high selectivity and yields (Figure 6b). Moreover, Ru@PGS proved to be reusable and robust in this case as well (Figure S17). Times profiles evidenced fast heteroaromatic and arene hydrogenation under H₂ (Figure 6c), while arene hydrogenation was almost completely shut down under H₂/CO₂ (Figure 6d). The behavior of Ru@PGS observed for benzofuran derivatives thus appears to be fully transposable to the hydrogenation of quinoline. After optimization of the reaction conditions (Table S11), a scope of quinoline derivatives (**7a–17a**) could be hydrogenated to give selectively decahydroquinolines (**7d–17d**, 53–99 % yield) and tetrahydroquinolines (**7b–17b**, 86–99 % yield) in high yields in the absence and presence of CO₂ in the feed gas, respectively (Table 3). Noticeably, arene ring hydrogenation was found slower for 6-(trifluoromethyl)quinoline (**16a**) than for 6-methylquinoline (**10a**), suggesting a strong influence of the substituents' electronic properties. Decahydroquinolines and tetrahydroquinolines are widely used in the synthesis of various drug molecules. For example, **15d** is an important building block entering in the preparation of potent histone deacetylase inhibitors to suppress the growth of prostate cancer cells,^[3c] while **15b** can be used to prepare NPT-IIb which has intestinal phosphate transporter inhibitory action.^[15]

Conclusion

In conclusion, the adaptivity of Ru@PGS materials towards CO₂ as a molecular trigger was successfully applied to the catalytic hydrogenation of bicyclic heteroaromatics to completely or partially saturated products. While full hydrogenation of a variety of O- and N-heteroarenes was observed under pure H₂ as feed gas, the use of H₂/CO₂ led to the formation of ammonium formate species on the catalyst, thereby triggering a switch of selectivity with nearly complete suppression of arene hydrogenation activity. This switch was found to be rapid, robust and fully reversible, providing access to valuable products from benzofuran and quinoline substrates in a controllable and adaptive manner. For example, methyl octahydrobenzofuran-5-carboxylate (**4d**) or methyl 2,3-dihydrobenzofuran-5-carboxylate (**4b**), two important building blocks for the production of pharmaceuticals were obtained selectively from methyl benzofuran-5-carboxylate (**4**) using the same catalyst under H₂ and H₂/CO₂, respectively. The same controlled selectivity switch was demonstrated for decahydroquinoline **15d** and tetrahydroquinoline **15b** as important building blocks for the preparation of different potent receptor inhibitors. With the presented adaptive catalytic system, the respective products can be produced from the same starting material

over a single catalyst in the same reactor unit, simply by switching ON or OFF an additional CO₂ supply in the hydrogen feed gas. The broad application range of the present system emphasizes the general potential of adaptive catalytic systems to enable flexible production schemes on the basis of molecular control mechanisms.

Acknowledgements

The authors acknowledge financial support by the Max Planck Society and by the Deutsche Forschungsgemeinschaft (DFG, German Research Foundation) under Germany's Excellence Strategy - Exzellenzcluster 2186 "The Fuel Science Center" ID: 390919832. The authors would like to thank, Norbert Pfänder (MPI CEC) and Silvia Palm (MPI Kofo) for STEM-EDX and SEM-EDX analysis. The authors are also thankful to Annika Gurowski, Alina Jakubowski, and Justus Werkmeister (MPI CEC) for GC and GC-MS measurements. We acknowledge DESY (Hamburg, Germany), a member of the Helmholtz Association HGF, for the provision of experimental facilities. Parts of this research were carried out at PETRA III and we would like to thank Dr. Edmund Welter for assistance in using P65 Applied XAFS Beamline. The XAFS beamtime was allocated for proposal I-20211319. L.K. acknowledges Alexander von Humboldt Foundation for a postdoctoral fellowship and funding support. T.W. acknowledges support from the DFG (Heisenberg fellowship, project number 455238107) and thanks Nina Schröder and Dr. Igor d'Anciães Almeida Silva for support with recording the solid-state NMR spectra. Open Access funding enabled and organized by Projekt DEAL.

Conflict of Interest

The authors declare no conflict of interest.

Data Availability Statement

The data that support the findings of this study are available in the supplementary material of this article.

Keywords: Adaptivity • Bicyclic Heteroaromatics • CO₂ Responsive Support • Hydrogenation • Selectivity Switch

- [1] a) S. Mandal, S. Saha, C. K. Jana, *Org. Lett.* **2020**, 22, 4883; b) X. F. Wang, F. Guan, E. Ohkoshi, W. Guo, L. Wang, D. Q. Zhu, S. B. Wang, L. T. Wang, E. Hamel, D. Yang, L. Li, K. Qian, S. L. Morris-Natschke, S. Yuan, K. H. Lee, L. Xie, *J. Med. Chem.* **2014**, 57, 1390; c) M. Saitoh, J. Kunitomo, E. Kimura, Y. Hayase, H. Kobayashi, N. Uchiyama, T. Kawamoto, T. Tanaka, C. D. Mol, D. R. Dougan, G. S. Textor, G. P. Snell, F. Itoh, *Bioorg. Med. Chem.* **2009**, 17, 2017.
- [2] a) X. X. Huang, C. C. Zhou, L. Z. Li, Y. Peng, L. L. Lou, S. Liu, D. M. Li, T. Ikejima, S. J. Song, *Fitoterapia* **2013**, 91, 217; b) M. Heitbaum, R. Fröhlich, F. Glorius, *Adv. Synth. Catal.*

- 2010, 352, 357; c) F. Shen, Z. P. Zhang, J. B. Li, Y. Lin, L. Liu, *Org. Lett.* **2011**, 13, 568.
- [3] a) Z. Li, X. Wang, X. Xu, Q. Qiu, L. Jiao, W. Huang, H. Qian, *Chem. Biol. Drug Des.* **2015**, 86, 764; b) Z. Huang, Y. Liu, Y. Li, L. Xiong, Z. Cui, H. Song, H. Liu, Q. Zhao, Q. Wang, *J. Agric. Food Chem.* **2011**, 59, 635; c) Y. M. Liu, H. Y. Lee, C. H. Chen, C. H. Lee, L. T. Wang, S. L. Pan, M. J. Lai, T. K. Yeh, J. P. Liou, *Eur. J. Med. Chem.* **2015**, 89, 320; d) Z. Wang, C. Fraley, A. R. Mezo, *Bioorg. Med. Chem. Lett.* **2013**, 23, 1253.
- [4] a) R. Adam, J. R. Cabrero-Antonino, A. Spannenberg, K. Junge, R. Jackstell, M. Beller, *Angew. Chem. Int. Ed.* **2017**, 56, 3216; b) W. Liu, B. Sahoo, K. Junge, M. Beller, *Acc. Chem. Res.* **2018**, 51, 1858; c) V. Papa, Y. Cao, A. Spannenberg, K. Junge, M. Beller, *Nat. Catal.* **2020**, 3, 135; d) Á. Vivancos, M. Beller, M. Albrecht, *ACS Catal.* **2017**, 8, 17; e) J. Fidalgo, M. Ruiz-Castaneda, G. Garcia-Herbosa, A. Carbayo, F. A. Jalon, A. M. Rodriguez, B. R. Manzano, G. Espino, *Inorg. Chem.* **2018**, 57, 14186; f) N. Ortega, S. Urban, B. Beiring, F. Glorius, *Angew. Chem. Int. Ed.* **2012**, 51, 1710; g) N. Ortega, B. Beiring, S. Urban, F. Glorius, *Tetrahedron* **2012**, 68, 5185; h) Q.-H. Fan, Y.-M. He, F.-J. Li in *Asymmetric Hydrogenation and Transfer Hydrogenation* (Eds.: V. Ratovelomanana-Vidal, P. Phansavath), Wiley-VCH, Weinheim, **2021**, pp. 255–279; i) D. Moock, T. Wagener, T. Hu, T. Gallagher, F. Glorius, *Angew. Chem. Int. Ed.* **2021**, 60, 13677.
- [5] a) F. Chen, A. E. Surkus, L. He, M. M. Pohl, J. Radnik, C. Topf, K. Junge, M. Beller, *J. Am. Chem. Soc.* **2015**, 137, 11718; b) S. El Sayed, A. Bordet, C. Weidenthaler, W. Hetaba, K. L. Luska, W. Leitner, *ACS Catal.* **2020**, 10, 2124; c) G. Li, H. Yang, H. Zhang, Z. Qi, M. Chen, W. Hu, L. Tian, R. Nie, W. Huang, *ACS Catal.* **2018**, 8, 8396; d) M. Puche, L. Liu, P. Concepción, I. Sorribes, A. Corma, *ACS Catal.* **2021**, 11, 8197; e) S. Rengshausen, C. Van Stappen, N. Levin, S. Tricard, K. L. Luska, S. DeBeer, B. Chaudret, A. Bordet, W. Leitner, *Small* **2021**, 17, 2006683; f) H.-Y. Jiang, X.-X. Zheng, *Appl. Catal. A* **2015**, 499, 118; g) A. Karakulina, A. Gopakumar, I. Akcok, B. L. Roulier, T. LaGrange, S. A. Katsyuba, S. Das, P. J. Dyson, *Angew. Chem. Int. Ed.* **2016**, 55, 292; h) A. Karakhanov, E. A. Viktorova, *Chem. Heterocycl. Compd.* **1976**, 12, 367.
- [6] a) A. Bordet, W. Leitner, *Angew. Chem. Int. Ed.* **2023**, 62, e202301956.
- [7] a) V. Blanco, D. A. Leigh, V. Marcos, *Chem. Soc. Rev.* **2015**, 44, 5341; b) J. Choudhury, *Tetrahedron Lett.* **2018**, 59, 487; c) I. Vassalini, I. Alessandri, *Catalysts* **2018**, 8, 569; d) M. Vlatković, B. S. Collins, B. L. Feringa, *Chem. Eur. J.* **2016**, 22, 17080; e) Y. P. Tang, Y. E. Luo, J. F. Xiang, Y. M. He, Q. H. Fan, *Angew. Chem. Int. Ed.* **2022**, 61, 202200638; f) S. Park, S. Byun, H. Ryu, H. Hahm, J. Lee, S. Hong, *ACS Catal.* **2021**, 11, 13860.
- [8] A. Bordet, S. El Sayed, M. Sanger, K. J. Boniface, D. Kalsi, K. L. Luska, P. G. Jessop, W. Leitner, *Nat. Chem.* **2021**, 13, 916.
- [9] K. J. Boniface, R. R. Dykeman, A. Cormier, H. B. Wang, S. M. Mercer, G. J. Liu, M. F. Cunningham, P. G. Jessop, *Green Chem.* **2016**, 18, 208.
- [10] a) A. Bordet, W. Leitner, *Acc. Chem. Res.* **2021**, 54, 2144; b) A. Bordet, G. Moos, C. Welsh, P. Licence, K. L. Luska, W. Leitner, *ACS Catal.* **2020**, 10, 13904.
- [11] Y.-P. Sun, H.-Y. Fu, D.-I. Zhang, R.-X. Li, H. Chen, X.-J. Li, *Catal. Commun.* **2010**, 12, 188.
- [12] L. Hu, X.-Y. Wei, Y.-H. Kang, X.-H. Guo, M.-L. Xu, Z.-M. Zong, *J. Energy Inst.* **2021**, 96, 269.
- [13] C. Fischer, S. L. Bogen, M. L. Childers, F. X. F. Llinas, J. M. Ellis, S. Esposito, D. M. Hoffman, C. Huang, S. D. Kattar, A. J. Kim, J. W. Lampe, M. R. Machacek, D. R. McMasters, J. D. L. Parker, M. I. H. Reutershan, Nu. Sciammetta, P. P. Shao, D. L. Sloman, W. Sun, F. Ujjainwalla, Z. Wu, Y. Yu, C. R. Gibeau, US010508108B2, **2015**.
- [14] D. S. Wang, Q. A. Chen, S. M. Lu, Y. G. Zhou, *Chem. Rev.* **2012**, 112, 2557.
- [15] S. Hachiya, M. Miura, Y. Imamura, D. Kaga, I. Sato, H. Moritomo, K. Kato, K. Terai, Y. Terada, US20130053369A1, **2012**.

Manuscript received: August 7, 2023

Accepted manuscript online: September 7, 2023

Version of record online: September 18, 2023